# Pyrolysis of Methyl *tert*-Butyl Ether (MTBE). 1. Experimental Study with Molecular-Beam Mass Spectrometry and Tunable Synchrotron VUV Photoionization

**Taichang Zhang, Jing Wang, Tao Yuan, Xin Hong, Lidong Zhang, and Fei Qi***

*National Synchrotron Radiation Laboratory, University of Science and Technology of China, Hefei, Anhui 230029, P. R. China*

*Received: April 25, 2008; Revised Manuscript Received: August 12, 2008*

An experimental study of methyl *tert*-butyl ether (MTBE) pyrolysis (3.72% MTBE in argon) has been performed at low pressure (267 Pa) within the temperature range from 700 to 1420 K. The pyrolysis process was detected with the tunable synchrotron vacuum ultraviolet (VUV) photoionization and molecular-beam mass spectrometry (MBMS). About thirty intermediates are identified from near-threshold measurements of photoionization mass spectrum and photoionization efficiency spectrum. Among them, $H_2$, CO, $CH_4$, $CH_3OH$ and $C_4H_8$ are the major pyrolysis products. The radicals such as methyl, methoxy, propargyl, allyl, $C_4H_5$ and $C_4H_7$ are detected. The isomers of pyrolysis products are identified as well, i.e., propyne and allene, 1,2,3-butatriene and vinylacetylene, isobutene and 1-butene, propanal and acetone. Furthermore, the mole fractions of the pyrolysis products have been evaluated under various temperatures. Meanwhile, the initial formation temperatures of different pyrolysis products can be obtained. This work is anticipated to present a new experimental method for pyrolysis study and help understand the pyrolysis and combustion chemistry of MTBE and other oxygenated fuels.

## 1. Introduction

Pyrolysis is a key process in combustion. Most combustion intermediates are derived from the pyrolysis process, especially for the primary degradation products of fuel and hydrocarbon subsequent growth processes. Moreover, the pyrolysis of fuels (such as benzene, toluene, methyl *tert*-butyl ether (MTBE), isooctane, *n*-heptane and JP-10) has been studied by different groups with various methods, such as flow tube,[1−7] shock tube,[8−16] and Knudsen cell.[17,18] It is noticeable that most previous investigations adopted electron-impact ionization mass spectrometry (EIMS) and/or gas chromatography (GC) to detect pyrolysis products. The limited energy resolution of ionizing electrons and fragmental interference preclude the identification of radicals and isomeric species for EIMS, whereas reactive molecules such as radicals can hardly be observed by the GC method. More recently, O'Keeffe and co-workers studied the thermal decomposition of azidoacetone using molecular-beam EIMS.[19]

MTBE is the most commonly used gasoline additive, in view of its excellent antiknock characteristics,[20] cost-effective, good emission reduction of carbon monoxide, ozone, benzene and other toxic hydrocarbons,[21] and efficiency improvement of internal combustion engine. Due to its undesirable property of water solubility, the leakage of MTBE is a potential contaminant to groundwater and human body. So its use is eliminated or limited in USA. But it is still used frequently in Europe and Asia. New degradation methods will decrease the threat.[22,23] Moreover, the study of the high temperature chemistry of MTBE will improve the understanding of the influence of the MTBE molecular structure on its many excellent characteristics, which may be helpful to find out more useful additives. Its oxidation[24−29] and combustion[30,31] have been extensively studied before. But unfortunately there have been few comprehensive studies of MTBE pyrolysis, which is crucial for understanding the high temperature chemistry of MTBE and extending our knowledge of selecting gasoline additives.

Choo et al. investigated the thermal decomposition of MTBE at very low pressures ($4.9 \times 10^{-3}$−$4.9 \times 10^{-1}$ Pa) and relative low temperature 800 K,[1] where primary pyrolysis is dominant. Secondary pyrolysis can become more important in fuel-rich conditions, but previous study of the secondary pyrolysis was scarce. Chambreau et al. studied the pyrolysis products of MTBE using photoionization mass spectrometry at the VUV wavelength of 118 nm.[2] Major products and few minor products were detected in the previous investigations. Moreover, less effort has been made to distinguish the isomeric intermediates.

Recently, the molecular-beam mass spectrometric technique coupled with tunable synchrotron VUV photoionization has been introduced in premixed flames.[32−39] The high energy resolution and broad energy tunability of synchrotron VUV light can help distinguish most isomers and reduce fragmentation via near-threshold photoionization, which enables the unambiguous detection of intermediates. For example, this method can identify radicals and isomers (e.g., enols and aldehydes) in hydrocarbon flames.[32,35,36] Here, we report an experimental study of MTBE pyrolysis using molecular-beam mass spectrometry (MBMS) and tunable synchrotron VUV photoionization. Benefiting from the broad tunability of synchrotron light, this new method is anticipated to provide a full picture of the pyrolysis process of MTBE, including the comprehensive observation of pyrolysis species and detailed measurements of their mole fraction profiles.

## 2. Experimental Method

The experimental work was carried out at National Synchrotron Radiation Laboratory (NSRL) in Hefei, China. Two beamlines were used for this study. One is a newly constructed beamline using undulator radiation from the 800 MeV electron

* Corresponding author. E-mail: fqi@ustc.edu.cn. Fax: +86-551-5141078. Tel: +86-551-3602125.

10.1021/jp803622w CCC: $40.75 
Published on Web 09/30/2008

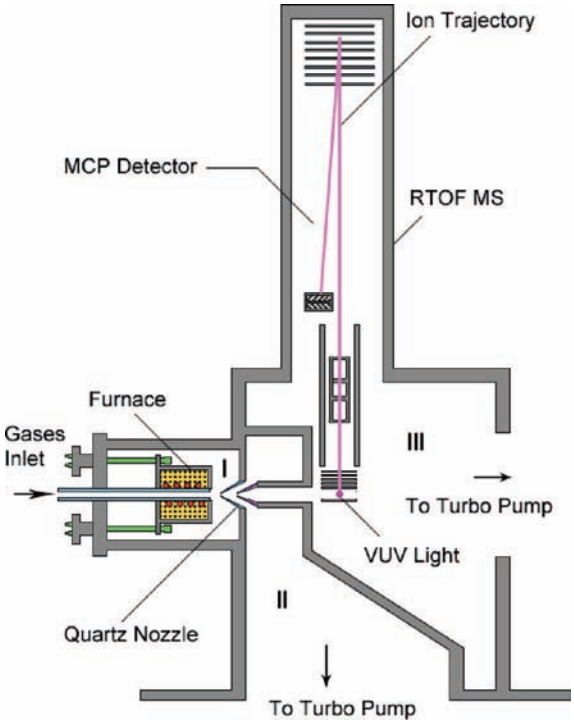


**Figure 1.** Schematic diagram of pyrolysis apparatus with molecular-beam sampling mass spectrometer. Regions **I**, **II** and **III** are the pyrolysis chamber, the differential pumped chamber, and the photoionization chamber, respectively. The synchrotron VUV light crosses vertically with the molecular beam and the ion trajectory, as indicated in the figure.

storage ring. Synchrotron radiation is dispersed by a 1 m Seya-Namioka monochromator equipped with a laminar grating (1500 grooves/mm, Horiba Jobin Yvon) covering the photon energies from 7.80 to 24.00 eV. The monochromator is calibrated with the known ionization energies of the inert gases. The energy resolving power ($E/\Delta E$) is about 1000. The average photon flux can reach the magnitude of $10^{13}$ photons/s. A gas filter is used to eliminate higher-order harmonic radiation with Ne or Ar filled in the gas cell. The other beamline utilizes radiation from a bending magnet with the photon energy range from 6.90 to 11.81 eV, which has been described in detail previously.[37] A LiF window is used to eliminate higher-order harmonic radiation. A silicon photodiode (SXUV-100, International Radiation Detectors, Inc.) is used to monitor the photon flux for normalizing ion signals.

As shown in Figure 1, the experimental setup consists of a pyrolysis chamber (**I**) with a high temperature furnace, a differentially pumped chamber (**II**) with a molecular-beam sampling system, and a photoionization chamber (**III**) with a reflectron time-of-flight mass spectrometer (RTOF-MS). The photoionization chamber and the differential chamber are pumped by two turbomolecular pumps with pumping speeds of 600 and 1500 L/s, respectively. A 15 L/s mechanical pump backs the turbopump of the photoionization chamber, and a 15 L/s mechanical pump plus a 70 L/s roots pump back the turbopump of the differential chamber. The pyrolysis chamber is pumped with a 27 L/s mechanical pump plus a 70 L/s roots pump. A quartz cone-like nozzle with a ~500 $\mu$m orifice at the tip is used to sample the pyrolysis species, including the reactant (MTBE), products, and intermediates. The sampled pyrolysis species form a molecular beam in the differentially pumped chamber and pass into the photoionization chamber through a nickel skimmer. Then, the molecular beam is crossed by the tunable synchrotron VUV light in the ionization region. Photoions produced by the VUV light are drawn out of the photoionization region by a pulse extraction field triggered with a pulse generator (DG 535, SRS), and then the ions are detected by a microchannel plate (MCP) detector. The ion signal is recorded by a multiscaler (P7888, FAST Comtec) after it is amplified with a preamplifier VT120C (EG & G, ORTEC).[40]

With the variation of photon energy, a series of mass spectra can be taken at the specified temperature for measurements of photoionization efficiency (PIE) spectra. The integrated ion intensity for a specific mass is normalized by the photon flux and plotted as a function of the photon energy, which then yields a PIE spectrum containing precise information of ionization energies (IEs) of corresponding species. In this work the PIE spectra have been measured at the pyrolysis temperature of 1380 K. Considering the cooling effect of molecular beam,[41] the experimental error for determined IEs is within 0.05 eV. To keep near-threshold ionization and avoid fragmentation, we scanned the temperature at some selected photon energies for evaluation of mole fractions.

The mixture of MTBE and Ar is fed into a 3-mm-ID (inside diameter) and 300-mm-length alumina flow tube with 100 mm inside the furnace. MTBE is diluted with Ar, which is controlled by a MKS mass flow controller with the flow rate of 0.50 standard liter per minute (SLM). And MTBE is controlled by a syringe pump (ISCO 1000D) with the liquid flow rate of 0.10 mL/min (equivalent to 0.0193 SLM in gas phase) at room temperature. After the syringe pump, MTBE is vaporized and mixed with Ar in a vaporizer with a temperature of 360 K. Thus, the total flow rate is 0.5193 SLM, and the inlet mole fraction of MTBE is calculated to be 3.72%. To reduce collisions of the pyrolysis species and detect the primary and secondary products containing radicals, the pressure of the pyrolysis chamber was kept at 267 Pa in this work, which was controlled by a MKS throttle valve. The temperature was measured by a Pt−30% Rh/Pt−6% Rh thermocouple inserted into the heating region inside the flow tube. The temperature uncertainty is within 50 K.

## 3. Flow Conditions in Pyrolysis Zone

The flow conditions are evaluated by using pure Ar. Because the Ar concentration is much higher than that of the MTBE sample, the conditions should be essentially similar to the sample-laden flow. The detailed calculation and discussion can be found in the Supporting Information; only a brief description and some results are shown below. When the flow rate of pure Ar is 0.5193 SLM (mass flow rate = 2.18 $Kg \cdot s^{-1} \cdot m^{-2}$), which equals the total flow rate of diluted Ar and MTBE in this work, the Reynolds number ($Re$) of the flow is calculated to be 308.2−110.6 over the temperature range from 298 to 1420 K. In view of $Re < 2000$, the flow can be considered as a laminar one.

The standard isothermal compressible flow equations with appropriate parameters can be used to calculate the pressure, flow characteristics and residence time of flow reactor.[42,43] As shown in Figure 2, the pressure, density, velocity of midpoint of the pyrolysis zone (i.e., 50 mm upstream from the exit of flow tube) as well as the residence time are dependent on the temperature. Among them, the pressure and velocity increase by about a factor of 1.4 with the increase of temperature, whereas both the density and residence time decrease by about a factor of 1.4. It should be pointed out that actually the pressure at the exit port is slightly higher than that in the pyrolysis chamber, which could cause the results deduced from above

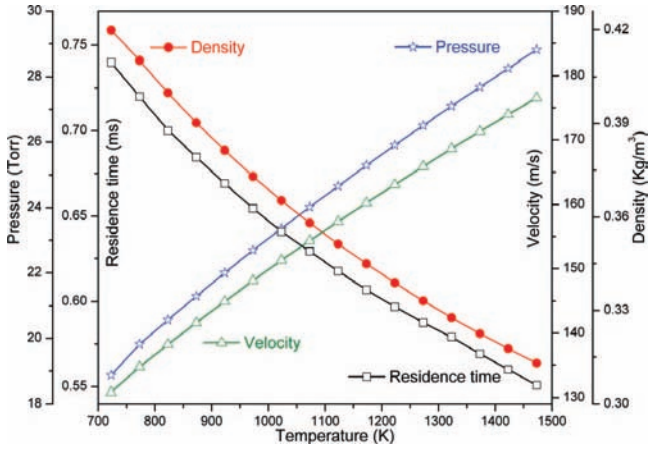


**Figure 2.** Temperature dependence of the pressure, density, and velocity of midpoint of the pyrolysis zone, as well as residence time, in the pyrolysis zone.

evaluations (pressure, density and residence time) a little lower. This is accordant with the practical situation. At 298 K the measured pressure at 300 mm upstream from the exit of the flow tube is 2670 Pa, which is slightly lower than the calculated pressure (2790 Pa).

The diffusion length $\langle r \rangle$, which is the root-mean-square (rms) displacement along one-dimension (radial) of an individual MTBE molecule as it randomly walks through Ar, is evaluated to be about 3 mm over the temperature range from 700−1420 K. For most MTBE molecules, $\langle r \rangle$ is large enough to cause at least one collision on the wall during the residence time, so the wall catalyzed effect cannot be ignored in our experimental conditions. That is, both homogeneous and heterogeneous reactions occur in the pyrolysis process. However, the collision between MTBE and Ar is dominant; thus there is minor contribution from the wall reaction. Moreover, after the experiment runs for a while, the carbon deposited on the internal wall of the flow tube may passivate the wall.

## 4. Results and Discussion

**4.1. Identification of Pyrolysis Species.** In this work, the results are mainly deduced from the measurements of photoionization mass spectra. Figure 3 shows a series of partial mass spectra taken at a temperature of 1420 K and the different photon energies labeled on the figure. A number of peaks with $m/z$ = 15−58 can be observed at the photon energy 11.81 eV, which belong to C to $C_4$ hydrocarbons. With the decrease of photon energy, the number of peaks also reduces. Furthermore, isomeric identification of pyrolysis species can be performed by the measurements of PIE spectra. For example, Figures 4 and 5 display PIE spectra of some intermediates formed in the pyrolysis of MTBE.

A clear onset at 9.82 eV on the PIE spectrum of $m/z$ = 15 in Figure 4a corresponds to ionization of the methyl radical (IE = 9.84 eV[44]). Similarly, an onset on the PIE spectrum of $m/z$ = 31 is located at 10.76 eV, as shown in Figure 4b, which corresponds to the IE of methoxy radical (IE = 10.72 eV[44]). The signal increases sharply around 11.60 eV, which includes the contribution from fragmentation of methanol. Figure 5a represents the PIE spectrum of $m/z$ = 32. The onset is located at 10.82 eV, which corresponding to ionization of methanol (IE = 10.84 eV[44]). Methanol is one of the major stable products in the MTBE pyrolysis, which will be discussed below. There are two possible isomers for $C_3H_4$ ($m/z$ = 40), that is, allene (IE = 9.69 eV[44]) and propyne (IE = 10.36 eV[44]). Figure 5b shows

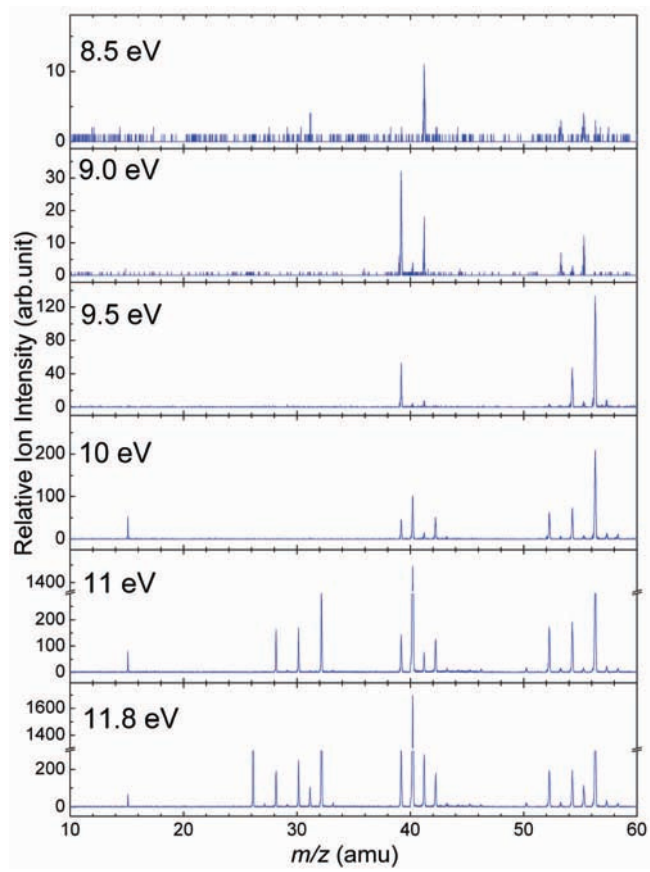


**Figure 3.** Photoionization mass spectra of MTBE pyrolysis taken at the temperature of 1420 K and different photon energies as labeled in the figure.

two clear onsets on the PIE spectrum of $m/z$ = 40, implying both allene and propyne formed in the pyrolysis of MTBE. The solid curve in Figure 5b presents the relative photoionization cross section simulated for a best-fit isomeric composition of 20 ± 5% allene and 80 ± 5% propyne (the photoionization cross section data for pure propyne and allene are reported by Cool et al.[38]) and has the similar trend of the PIE spectrum measured in the pyrolysis of MTBE. One clear onset at 9.68 eV is observed in the PIE spectrum of $m/z$ = 58, which corresponds to ionization of acetone (IE = 9.70 eV[44]). But the difference between the experimental data and the PIE spectrum of acetone can be found above 9.95 eV, which implies that another isomer could contribute to the measured PIE spectrum. After considering contribution of propanal (IE = 9.96 eV[44]) to the PIE spectrum, the experimental data are in good agreement with the simulated curve for isomeric composition of 53 ± 5% acetone and 47 ± 5% propanal below the photon energy of 10.68 eV, as shown in Figure 5c. There still exists a difference between the simulated curve and the experimental data above 10.68 eV, which corresponds to contribution of ionization of isobutane (IE = 10.68 eV[44]). Similarly, mass 56 includes three species of isobutene (IE = 9.22 eV[44]), 1-butene (IE = 9.55 eV[44]) and 2-propenal (IE = 10.11 eV[44]), as shown in Figure 5d. Here only a few PIE spectra are selected to explain isomeric identification for pyrolysis study. The intermediates and products identified in this work are listed in Table 1 with their IEs. For the species with trace level, their IEs are not listed in the table.

**4.2. Mole Fraction Evaluation.** The mole fraction of observed pyrolysis species versus the pyrolysis temperature can be evaluated from the measurements of near-threshold photoionization mass spectra taken at different temperatures, as shown

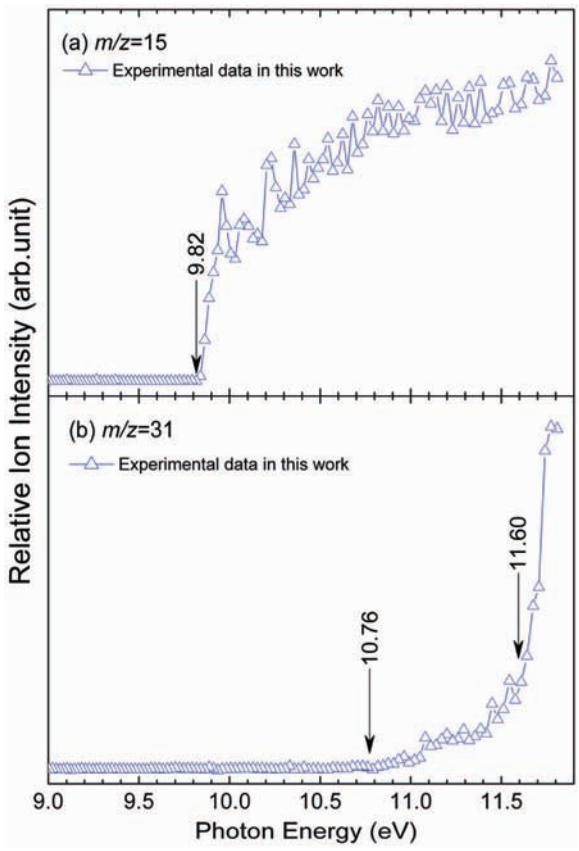


**Figure 4.** (a) PIE spectrum of $m/z = 15$ and (b) PIE spectrum of $m/z = 31$ from pyrolysis of MTBE.

in Figure 6. Ar is used as the reference species for mole fraction evaluation in this work due to its inert chemical property. Because the pressure keeps constant at the sampling position, the variation of Ar signals with increasing temperature is mainly caused by various reasons, including the gas expansion at the high temperature, distance between nozzle and the furnace, and the variation of total gaseous molecular number caused by pyrolysis. In this work, the total influence is defined as the gas expansion coefficient $\lambda(T)$, which should be identical for all pyrolysis species. $\lambda(T)$ can be presented from the measurements of Ar signal as a function of temperature, as shown in Figure 7. The gas expansion coefficient $\lambda(T)$ indicates a monotonous decrease between 700 and 1420 K. However, it is possible that expansion effects are mass dependent. Fortunately, in the present case only significant effect might be for $H_2$, which will tend to scatter out of molecular beam due to its light mass. The mole fraction evaluation for $H_2$ is special, presented below in detail. Cool et al. described a method for mole fraction evaluation, which is mainly applied to low-pressure premixed flame.[45] Basing on the method by Cool et al., a modified method is introduced for pyrolysis study in this work.

For species $i$, the ion signal ($S_i$) is written as the following equation,

$$S_i(T,E) = C \times X_i(T,E) \times \sigma_i(E) \times D_i \times \Phi_p(E) \times \lambda(T) \quad (1)$$

Here $C$ is a proportional constant, $X_i(T,E)$ is the mole fraction of species $i$ at the temperature $T$ and photon energy $E$, $\sigma_i(E)$ is the photoionization cross section of the species $i$ at the photon energy $E$, $D_i$ is the mass discrimination factor for the species $i$, $\Phi_p(E)$ is the photon flux. Thus, for the fixed photon energy and photon flux, the mole fraction of MTBE at the temperature $T$ can be evaluated by eq 2,

$$X_{MTBE}(T,E) = X_{MTBE}(T_1,E) \times S_{MTBE}(T,E)/S_{MTBE}(T_1,E)/\lambda(T) \quad (2)$$

$S_{MTBE}(T_1,E)$ and $X_{MTBE}(T_1, E)$ represent the initial ion signal and the inlet mole fraction of MTBE before its decomposition. In this study, $T_1$ is defined as 700 K for MTBE, which means that the pyrolysis process just begins at this temperature. $X_{MTBE}(T_1\ E)$ is 3.72%. However, MTBE is ready to dissociate to the fragments $C_4H_9O^+$ ($m/z = 73$) and $C_4H_9^+$ ($m/z = 57$) at the photon energy of 11.81 eV, as shown in Figure 6. The ion signal profile of $m/z = 73$ versus the pyrolysis temperature has the same tendency as that of MTBE cation. Thus the mole fraction of MTBE is derived from the data of $m/z = 73$ in this work.

Then the mole fraction of $C_2H_2$ can be calculated by eq 3,

$$X_{C_2H_2}(T)/X_{Ar} = [S_{C_2H_2}(T,E')/S_{Ar}(T,E')] \times [\sigma_{Ar}(E')/\sigma_{C_2H_2}(E')] \times [D_{Ar}/D_{C_2H_2}] \quad (3)$$

In the above equation, $E'$ is 16.00 eV. Furthermore, mole fractions of hydrocarbon species can be calculated by eq 4,

$$X_i(T)/X_{C_2H_2}(T) = [S_i(T,E)/S_{C_2H_2}(T,E)] \times [\sigma_{C_2H_2}(E)/\sigma_i(E)] \times [D_{C_2H_2}/D_i] \quad (4)$$

$D_i$ was measured and is presented as Figure S1 in the Supporting Information. Photoionization cross sections of some small hydrocarbons can be found in the literature.[38,46−49] To reduce the uncertainty of mole fraction evaluation in this work, we measured the value of $\sigma_i D_i$ for $H_2$, which is the most abundant product in this work. From the cold flow measurements of the binary mixture of $H_2$ and Ar, the ion signal ratio of $H_2$ to Ar can be directly obtained to calculate the value of $\sigma_i D_i$. Because the elements C, H and O are kept as a constant, the hydrogen element balance was employed to normalize the total mole fractions of pyrolysis species, leading to an estimated uncertainty within 30% (see Figure S2 in the Supporting Information).

**4.3. Mole Fraction Profiles and Decomposition Pathways.** In this study, photon energies of 16.00, 15.00, 13.00, 11.81, 11.50, 11.00, 10.00, 9.50 and 8.50 eV are selected for the measurements of temperature scan to get near-threshold photoionization of all observed pyrolysis species. The initial formation temperatures ($T_F$), the maximum mole fractions ($X_M$) and the corresponding temperatures ($T_M$) of some intermediates are also listed in Table 1.

About thirty pyrolysis species have been observed in this work, whose mole fraction profiles are presented in Figures 8 and 9. The mole fraction profiles of MTBE, major products ($H_2$, CO, $CH_4$, $CH_3OH$ and $C_4H_8$) are illustrated in Figure 8. MTBE begins to decompose around 730 K, and its concentration decreases gradually from the initial value of 3.72% to full decomposition at 1400 K. The concentrations of CO and $H_2$ increase continuously with temperature increasing, and their $T_F$'s are 890 and 1060 K, respectively. The $T_F$'s of both $CH_3OH$ and $C_4H_8$ are 730 K. The maximum mole fractions of $CH_3OH$ and $C_4H_8$ are 2.31E−2 and 3.04E−2, respectively, at the temperature 1260 K. The $T_F$ of $CH_4$ is 940 K and its mole fraction reaches the peak at 1420 K.

Figure 9a shows mole fraction profiles of $C_1$ to $C_2$ intermediates including $CH_3$, $C_2H_2$, $C_2H_4$, $CH_2O$ and $CH_3O$. As seen from the figure, $T_F$'s of these species are in the range 850−1260 K, whereas their $T_M$'s are in the range 1220−1420 K. The mole fraction profiles of $C_3$ intermediates, including $C_3H_3$, $C_3H_4$ (allene and propyne), $C_3H_5$ and $C_3H_6$ are displayed in Figure

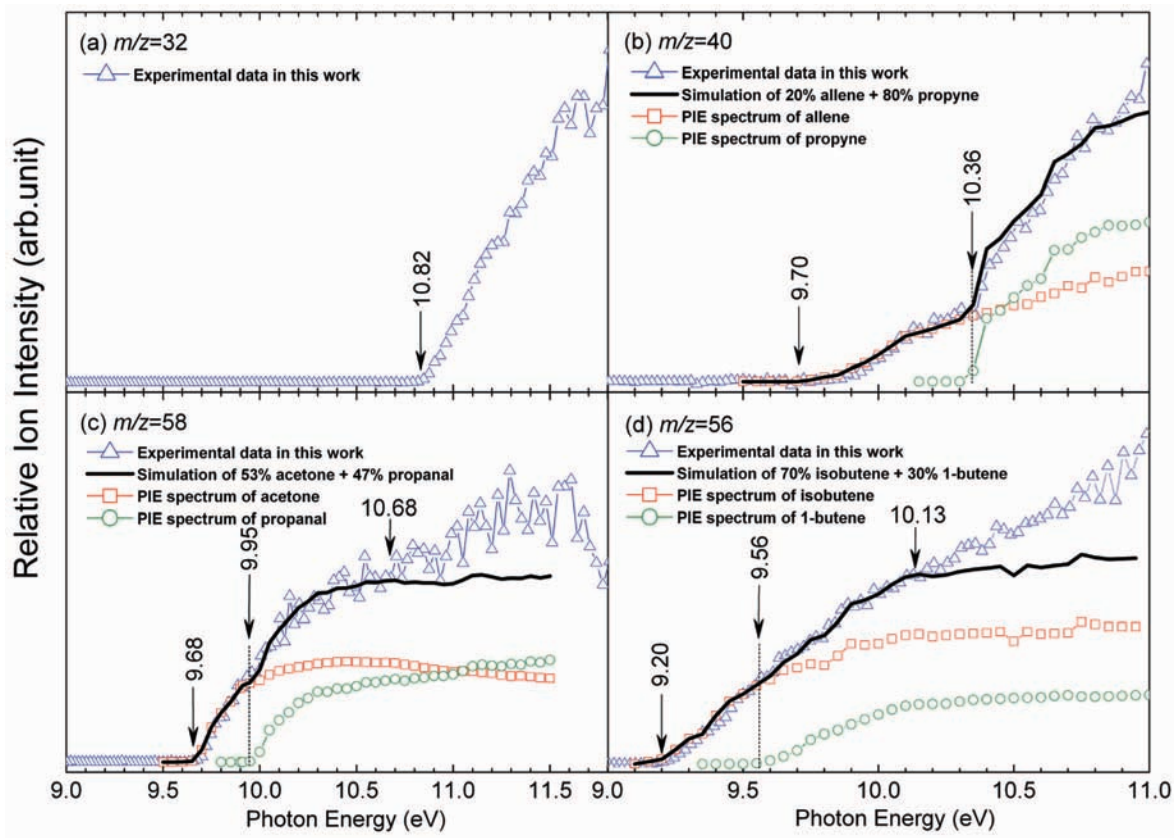


**Figure 5.** (a) PIE spectrum of $m/z = 32$ from pyrolysis of MTBE. (b) PIE spectrum of $m/z = 40$ measured from pyrolysis of MTBE, along with the simulated relative photoionization cross section (the solid line) for a mixture of 20 ± 5% allene and 80 ± 5% propyne. (c) PIE spectrum of $m/z = 58$ measured from pyrolysis of MTBE, along with the simulated relative photoionization cross section (the solid line) for a mixture of 53 ± 5% acetone and 47 ± 5% propanal. (d) PIE spectrum of $m/z = 56$ measured from pyrolysis of MTBE, along with the simulated relative photoionization cross section (the solid line) for a mixture of 70 ± 5% isobutene and 30 ± 5% 1-butene.

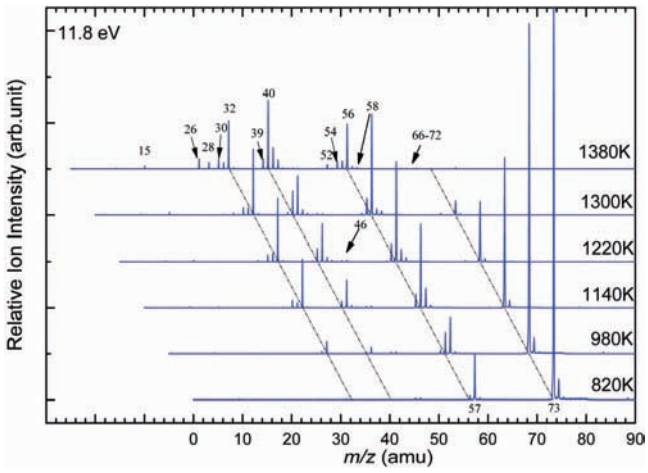


**Figure 6.** Stack plot of photoionization mass spectra of MTBE pyrolysis taken at the photon energy of 11.81 eV with different temperatures labeled in the figure.

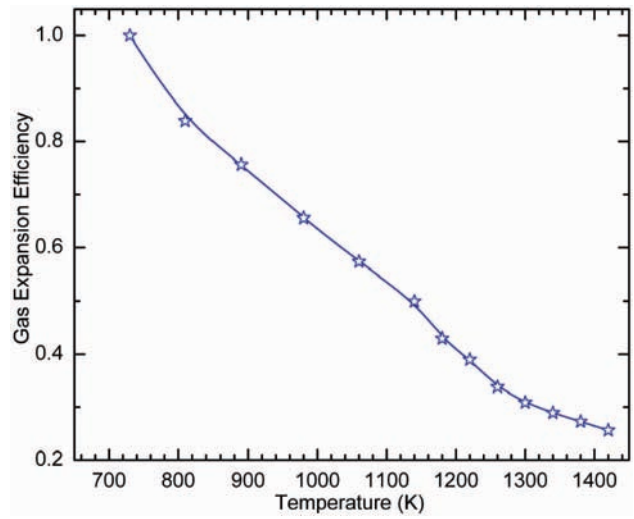


**Figure 7.** Gas expansion coefficient versus the pyrolysis temperature.

9b. $T_F$'s and $T_M$'s of these species are in the ranges 850−1260 and 1340−1420 K, respectively. Figure 9c shows mole fraction profiles of $C_4$ intermediates, including $C_4H_2$, $C_4H_4$, $C_4H_6$ and $C_4H_7$. The $T_F$'s of these species are in the range 980−1220 K, and the $T_M$'s are above 1380 K. The mole fraction profiles of $C_2H_6O$, $C_3H_6O$, $C_5H_6$, $C_5H_8$, $C_5H_{10}$ and $C_6H_6$ are displayed in Figure 9d with $T_F$'s and $T_M$'s in the ranges 850−1260 and 1260−1420 K.

The formation temperature of methanol and isobutene is around 730 K, which is lower than those of all other pyrolysis products. This is actually in good agreement with previous work that the most favorable pyrolysis pathway is the dissociation of MTBE to methanol and isobutene via a four-member-ring transition state.[1] When the pyrolysis temperature reaches around 900 K, propyne, methoxy radical, $H_2CO$, CO, $C_3H_6O$ and/or isobutane can be detected. Propyne can be formed via $CH_4$ abstraction from isobutene. The methoxy radical can be produced via H-elimination from methanol. However, the dissociation energy of methanol to the methoxy radical is very high.[50] Moreover the $T_F$ of $C_4H_7$ produced via the H-elimination

**TABLE 1: List of Intermediates Measured in the Pyrolysis of MTBE**

| | | | IE (eV) | | | | |
|---|---|---|---|---|---|---|---|
| *m/z* | formula | species | literature[a] | this work[b] | $X_M$[c] | $T_F$ (K)[d] | $T_M$ (K)[e] |
| 2 | $H_2$ | hydrogen | 15.43 | 15.43 | 1.84E−2 | 1060 | 1420 |
| 15 | $CH_3$ | methyl radical | 9.84 | 9.82 | 2.51E−3 | 940 | 1420 |
| 16 | $CH_4$ | methane | 12.61 | 12.60 | 1.57E−2 | 940 | 1420 |
| 26 | $C_2H_2$ | acetylene | 11.40 | 11.40 | 3.58E−3 | 1260 | 1420 |
| 28 | $C_2H_4$ | ethylene | 10.51 | 10.49 | 4.56E−3 | 980 | 1420 |
| | CO | carbon monoxide | 14.01 | 14.00 | 1.25E−2 | 890 | 1420 |
| 30 | $H_2CO$ | formaldehyde | 10.88 | 10.86 | 4.56E−3 | 850 | 1420 |
| 31 | $CH_3O$ | methoxy radical | 10.72 | 10.76 | 7.46E−5 | 890 | 1220 |
| 32 | $CH_3OH$ | methanol | 10.84 | 10.82 | 2.31E−2 | 730 | 1260 |
| 39 | $C_3H_3$ | propargyl radical | 8.67 | 8.65 | 1.37E−3 | 1260 | 1420 |
| 40 | $C_3H_4$ | propyne | 10.36 | 10.36 | 4.96E−3 | 850 | 1420 |
| | $C_3H_4$ | allene | 9.69 | 9.70 | 5.19E−3 | 980 | 1380 |
| 41 | $C_3H_5$ | allyl radical | 8.18 | 8.17 | 3.59E−4 | 1060 | 1340 |
| 42 | $C_3H_6$ | propylene | 9.73 | 9.71 | 2.31E−3[f] | 980[g] | 1380[g] |
| | $C_2H_2O$ | ketene | 9.62 | 9.64 | | | |
| 46 | $C_2H_6O$ | ethanol | 10.48 | 10.47 | 4.26E−4 | 1140 | 1300 |
| 50 | $C_4H_2$ | diacetylene | 10.17 | 10.16 | 7.89E−5 | 1220 | 1420 |
| 52 | $C_4H_4$ | 1,2,3-butatriene | 9.25 | 9.24 | 5.40E−4[f] | 1180[g] | 1420[g] |
| | $C_4H_4$ | vinylacetylene | 9.58 | 9.58 | | | |
| 53 | $C_4H_5$ | | | | <1.00E−5 | | |
| 54 | $C_4H_6$ | 1,3-butadiene | 9.07 | 9.08 | 2.25E−3 | 1060 | 1380 |
| 55 | $C_4H_7$ | | | | 7.24E−5 | 980 | 1380 |
| 56 | $C_3H_4O$ | 2-propenal | 10.11 | 10.13 | 3.04E−2[f] | 730[g] | 1260[g] |
| | $C_4H_8$ | isobutene | 9.22 | 9.20 | | | |
| | $C_4H_8$ | 1-butene | 9.55 | 9.56 | | | |
| 58 | $C_3H_6O$ | propanal | 9.96 | 9.95 | 1.07E−3[f] | 850[g] | 1260[g] |
| | $C_3H_6O$ | acetone | 9.70 | 9.68 | | | |
| | $C_4H_{10}$ | isobutane | 10.68 | 10.68 | | | |
| 66 | $C_5H_6$ | | | | 4.12E−5 | 1220 | 1420 |
| 68 | $C_5H_8$ | | | | 5.20E−5 | 1180 | 1380 |
| 70 | $C_5H_{10}$ | | | | 8.72E−5 | 980 | 1300 |
| 72 | $C_4H_8O$ | | | | <1.00E−5[f] | | |
| | $C_5H_{12}$ | | | | | | |
| 78 | $C_6H_6$ | | | | 8.73E−5 | 1260 | 1420 |

[a] Reference 18. [b] The uncertainty for IE is ±0.05 eV in this work. [c] The maximum mole fractions. [d] $T_F$ refers to the initial temperature for formation of species. [e] $T_M$ refers to the temperature relating to the maximum mole fraction.[44] [f] The value is the total maximum mole fraction of species with the same mass. [g] The value of all species with the same mass.

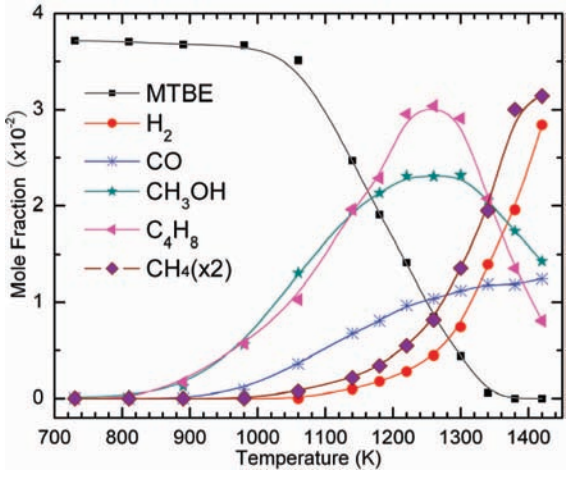


**Figure 8.** Mole fraction profiles of MTBE and major products ($CH_3OH$, $C_4H_8$, $CH_4$, CO and $H_2$). Symbols represent the mole fractions of corresponding species, and B-spline curves are used to connect the symbols.

from $C_4H_8$ is 980 K. It is known that the bond energy of a regular C−H is lower than that of O−H.[51] Thus there should be other pathways to form propyne and the methoxy radical. Among them, the direct dissociation of MTBE to the methoxy radical + *tert*-butyl radical is an important channel. This reaction provides not only one pathway of methoxy formation but also a new pathway of isobutene formation in the view of H-elimination of the *tert*-butyl radical. As shown in Figure 8, the mole fraction of isobutene is identical to that of methanol below 1150 K and is higher than that of methanol above 1150 K. The new channel of isobutene formation may play an important role at higher temperature.

MTBE can form $C_3H_6O$, undergoing a transition state or intermediate that is ready to further decompose, because intermediates related to $C_3H_6O$ are not detected at around 900 K in this experiment. At the same time, $CH_3/CH_4$ can be formed as well. But the $T_F$'s of both $CH_3$ and $CH_4$ are 940 K. Thus mass peak of $m/e = 58$ detected at 850 K is attributed to isobutane. There may be two pathways to form isobutane. One is dissociation of MTBE to isobutane + $H_2CO$, and the other is *tert*-butyl radical attacking stable intermediates and abstracting H. For the formation of $H_2CO$, there may be also two channels. One is mentioned above, and the other is H-elimination from methoxy radical. CO is one major product in this work; there are two major channels to form it. $H_2CO$ can form CO via $H_2$ abstraction and $C_3H_6O$ can undergo two steps of $CH_3$ abstraction to form CO. The former one is mainly at low temperature and the latter one competes with the former one at high temperature.

More and more attention is paid to the oxygen-containing fuels for their well-known advantages. However, poisonous compounds such as aldehydes are emitted in combustion of oxygen-containing fuel. Propanal and 2-propenal are detected

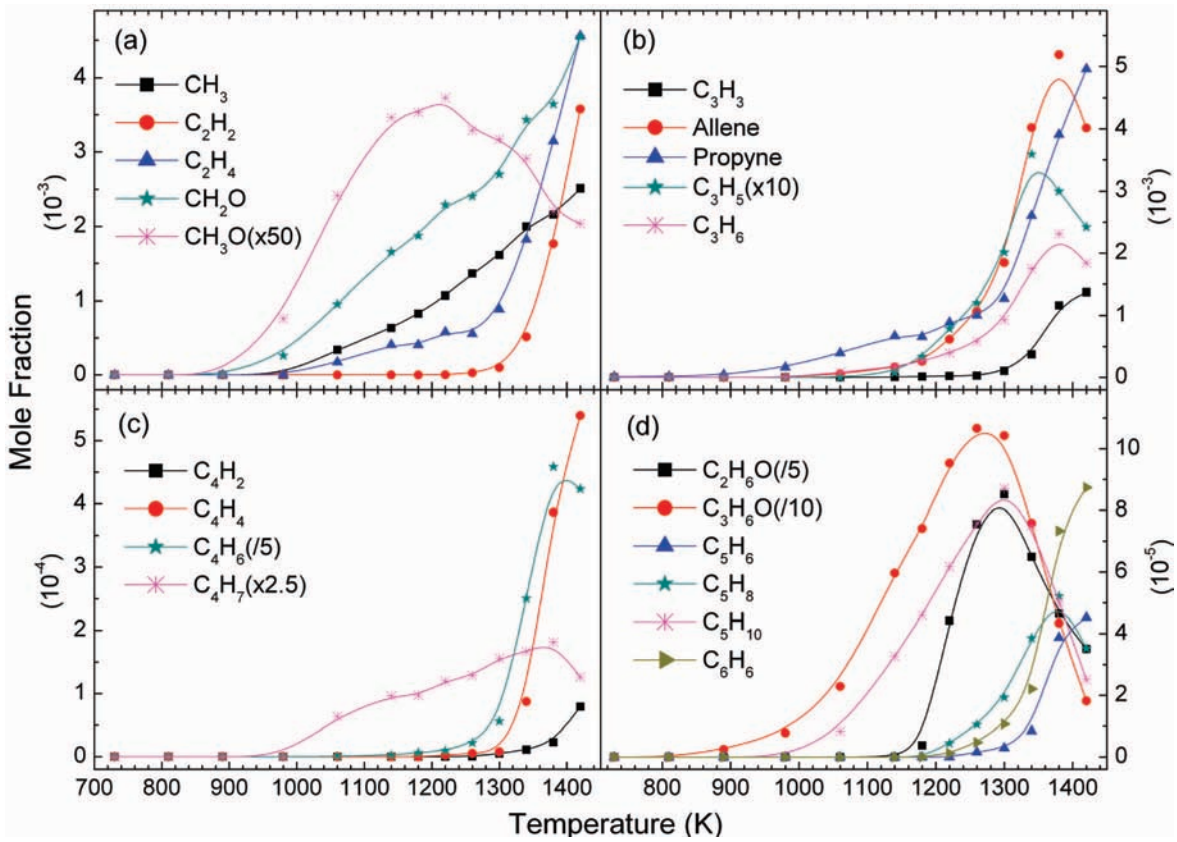


**Figure 9.** Mole fraction profiles of (a) C and $C_2$ intermediates, (b) $C_3$ intermediates, (c) $C_4$ intermediates, and (d) $C_2H_6O$, $C_3H_6O$, $C_5H_6$, $C_5H_8$, $C_5H_{10}$ and $C_6H_6$.

in our experiment. This indicates aldehydes can be formed by thermal decomposition of oxygen-containing fuel itself.

With the decrease of the H content in stable $C_4$ species, the mole fractions are found in the order of $C_4H_6 > C_4H_4 > C_4H_2$ and the $T_F$'s in the order $C_4H_6 < C_4H_4 < C_4H_2$, as seen in Table 1 and Figure 9. It indicates that $C_4$ species are formed via H abstraction/elimination step by step. Similarly, with the decrease of the H content in $C_5$ species, the mole fractions are found in the order $C_5H_{10} > C_5H_8 > C_5H_6$ and the $T_F$'s in the order $C_5H_{10} < C_5H_8 < C_5H_6$. Both $C_4$ and $C_5$ species present the same tendency for mole fraction and $T_F$'s. Moreover, the $T_F$'s of $C_5H_{10}$ and $C_4H_7$ are the same. All these indicate that $C_5$-species, containing $C_5H_6$, $C_5H_8$ and $C_5H_{10}$, are formed by recombination of methyl and $C_4H_3/C_4H_5/C_4H_7$, respectively. The specific isomers of mentioned-above $C_4$ and $C_5$ compounds are not identified in experiment due to insufficient signal intensity for PIE measurements, thus the specific compounds are not listed in Table 1. Besides $C_5$ species, benzene and methanol are also formed by combination of relative small intermediates. Two general pathways are accepted as benzene formation, self-combination of $C_3H_3$ and $C_2 + C_4$ species reactions. The amount of $C_4H_2$ in this work is not sufficient, thus the combination of $C_4H_2$ and $C_2H_4$ is not dominant. Ethanol is formed by combination of hydroxymethyl radical and methyl radical. The methyl radical plays an important role in the recombination of pyrolysis products. A detailed pyrolysis picture of MTBE is provided in the part 2 with theoretical calculation.[52]

## 5. Conclusion

Experimental study of MTBE pyrolysis has been performed with the tunable synchrotron VUV photoionization and molecular-beam mass spectrometry. Isomeric identification has been performed on the basis of the measurements of photoionization mass spectra and photoionization efficiency spectra, and mole fraction profiles are obtained by scanning the pyrolysis temperature at selected photon energies near ionization threshold. Compared with previous studies, more pyrolysis species have been detected in this work, especially radicals and isomers. Radicals such as the methyl, methoxy, propargyl and allyl radicals are identified. The isomers of pyrolysis products are also identified, i.e., propyne and allene, 1,2,3-butatriene and vinylacetylene, isobutene and 1-butene, propanal and acetone, etc. Among them, the concentration ratio of propanal/acetone at 1380 K almost reaches even, which indicates that the isomerization should be ubiquitous. As seen from mole fractions of pyrolysis products, most detected species are primary and secondary pyrolysis products, and a few recombination species including $C_5$ compounds, ethanol and benzene are produced with low concentration. Ethanol and $C_5$ species are formed by combination of methyl with $CH_2OH/C_4H_3/C_4H_5/C_4H_7$. The first pyrolysis pathway is the dissociation of MTBE to methanol and isobutene via a four-member-ring transition state. Besides, the direct dissociation of MTBE to methoxy radical + *tert*-butyl radical is another important pyrolysis pathway. Acetone can be formed by pyrolysis of MTBE at relative high temperature.

**Acknowledgment.** We gratefully acknowledge a reviewer for valuable suggestions on calculations of flow condition and diffusion length, and also Dr. Taohong Ye and Prof. Yiliang Chen for useful discussions. F.Q. is grateful for the funding supports from Chinese Academy of Sciences, the Specialized Research Fund for the Doctoral Program of Higher Education, Natural Science Foundation of China under Grant no. 20533040, National Basic Research Program of China (973) under Grant

no. 2007CB815204 and Ministry of Science and Technology of China under Grant no. 2007DFA61310.

**Supporting Information Available:** Full description of mass discrimination factor, the uncertainty of mole fraction, and evaluation of the flow condition. This material is available free of charge via the Internet at http://pubs.acs.org.

## References and Notes

(1) Choo, K. Y.; Golden, D. M.; Benson, S. W. *Int. J. Chem. Kinet.* **1974**, *6*, 631.
(2) Chambreau, S. D.; Zhang, J. S.; Traeger, J. C.; Morton, T. H. *Int. J. Mass Spectrom.* **2000**, *199*, 17.
(3) Slysh, R. S.; Kinney, C. R. *J. Phys. Chem.* **1961**, *65*, 1044.
(4) Badger, G. M.; Spotswood, T. M. *J. Chem. Soc.* **1960**, *218*, 4420.
(5) Shukla, B.; Susa, A.; Miyoshi, A.; Koshi, M. *J. Phys. Chem. A* **2007**, *111*, 8308.
(6) Pant, K. K.; Kunzru, D. *J. Anal. Appl. Pyrol.* **1996**, *36*, 103.
(7) Rao, P. N.; Kunzru, D. *J. Anal. Appl. Pyrol.* **2006**, *76*, 154.
(8) Laskin, A.; Lifshitz, A. *Proc. Combust. Inst.* **1996**, *26*, 669.
(9) Sivaramakrishnan, R.; Brezinsky, K.; Vasudevan, H.; Tranter, R. S. *Combust. Sci. Technol.* **2006**, *178*, 285.
(10) Astholz, D. C.; Durant, J.; Troe, J. *Proc. Combust. Inst.* **1980**, *18*, 885.
(11) Pamidimukkala, K. M.; Kern, R. D.; Patel, M. R.; Wei, H. C.; Kiefer, J. H. *J. Phys. Chem.* **1987**, *91*, 2148.
(12) Braun-unkhoff, M.; Frank, P.; Just, T. *Proc. Combust. Inst.* **1988**, *22*, 1053.
(13) Brouwer, L. D.; Muller-Markgraf, W.; Troe, J. *J. Phys. Chem.* **1988**, *92*, 4905.
(14) Eng, R. A.; Gebert, A.; Goos, E.; Hippler, H.; Kachiani, C. *Phys. Chem. Chem. Phys.* **2002**, *4*, 3989.
(15) Sivaramakrishnan, R.; Tranter, R. S.; Brezinsky, K. *J. Phys. Chem. A* **2006**, *110*, 9388.
(16) Davidson, D. F.; Oehlschlaeger, M. A.; Hanson, R. K. *Proc. Combust. Inst.* **2007**, *31*, 321.
(17) Smith, R. D.; Johnson, A. L. *Combust. Flame* **1983**, *51*, 1.
(18) Smith, R. D. *J. Phys. Chem.* **1979**, *83*, 1553.
(19) O'Keeffe, P.; Scotti, G.; Stranges, D.; Rodrigues, P.; Barros, M. T.; Costa, M. L. *J. Phys. Chem. A* **2008**, *112*, 3086.
(20) Papachristos, M. J.; Swithenbank, J.; Priestman, G. H.; Stournas, S.; Polysis, P.; Lois, E. *J. Inst. Energ.* **1991**, *64*, 113.
(21) Sawyer, R. F. *Pro. Combust. Inst.* **1992**, *24*, 1423.
(22) Deeb, R. A.; Scow, K. M.; Alvarez-Cohen, L. *Biodegradation* **2000**, *11*, 171.
(23) Haggblom, M. M.; Youngster, L. K. G.; Somsamak, P.; Richnow, H. H. *Adv. Appl. Microbiol.* **2007**, *62*, 1.
(24) Brocard, J. C.; Baronnet, F.; O'Neal, H. E. *Combust. Flame* **1983**, *52*, 25.
(25) Ciajolo, A.; Danna, A.; Kurz, M. *Combust. Sci. Technol.* **1997**, *123*, 49.
(26) Norton, T. S.; Dryer, F. L. *Proc. Combust. Inst.* **1991**, *23*, 179.
(27) Dunphy, M. P.; Simmie, J. M. *Combust. Sci. Technol.* **1989**, *66*, 157.
(28) Curran, H. J.; Dunphy, M. P.; Simmie, J. M.; Westbrook, C. K.; Pitz, W. J. *Proc. Combust. Inst.* **1992**, *24*, 769.
(29) Bohm, H.; Baronnet, F.; El Kadi, B. *Phys. Chem. Chem. Phys.* **2000**, *2*, 1929.
(30) Yao, C. D.; Li, J.; Li, Q.; Huang, C. Q.; Wei, L. X.; Wang, J.; Tian, Z. Y.; Li, Y. Y.; Qi, F. *Chemosphere* **2007**, *67*, 2065.
(31) Franklin, P. M.; Koshland, C. P.; Lucas, D.; Sawyer, R. F. *Chemosphere* **2001**, *42*, 861.
(32) Taatjes, C. A.; Hansen, N.; McIlroy, A.; Miller, J. A.; Senosiain, J. P.; Klippenstein, S. J.; Qi, F.; Sheng, L. S.; Zhang, Y. W.; Cool, T. A.; Wang, J.; Westmoreland, P. R.; Law, M. E.; Kasper, T.; Kohse-Höinghaus, K. *Science* **2005**, *308*, 1887.
(33) Yang, B.; Li, Y. Y.; Wei, L. X.; Huang, C. Q.; Wang, J.; Tian, Z. Y.; Yang, R.; Sheng, L. S.; Zhang, Y. W.; Qi, F. *Proc. Combust. Inst.* **2007**, *31*, 555.
(34) Yang, B.; Osswald, P.; Li, Y. Y.; Wang, J.; Wei, L. X.; Tian, Z. Y.; Qi, F.; Kohse-Höinghaus, K. *Combust. Flame* **2007**, *148*, 198.
(35) Yang, B.; Huang, C. Q.; Wei, L. X.; Wang, J.; Sheng, L. S.; Zhang, Y. W.; Qi, F.; Zheng, W. X.; Li, W. K. *Chem. Phys. Lett.* **2006**, *423*, 321.
(36) Hansen, N.; Klippenstein, S. J.; Taatjes, C. A.; Miller, J. A.; Wang, J.; Cool, T. A.; Yang, B.; Yang, R.; Wei, L. X.; Huang, C. Q.; Wang, J.; Qi, F.; Law, M. E.; Westmoreland, P. R. *J. Phys. Chem. A* **2006**, *110*, 3670.
(37) Qi, F.; Yang, R.; Yang, B.; Huang, C. Q.; Wei, L. X.; Wang, J.; Sheng, L. S.; Zhang, Y. W. *Rev. Sci. Instrum.* **2006**, *77*, 084101.
(38) Cool, T. A.; Nakajima, K.; Mostefaoui, T. A.; Qi, F.; McIlroy, A.; Westmoreland, P. R.; Law, M. E.; Peterka, D. S.; Ahmed, M. *J. Chem. Phys.* **2003**, *119*, 8356.
(39) Cool, T. A.; McIlroy, A.; Qi, F.; Westmoreland, P. R.; Poisson, L.; Peterka, D. S.; Ahmed, M. *Rev. Sci. Instrum.* **2005**, *76*, 094102.
(40) Huang, C. Q.; Yang, B.; Yang, R.; Wang, J.; Wei, L. X.; Shan, X. B.; Sheng, L. S.; Zhang, Y. W.; Qi, F. *Rev. Sci. Instrum.* **2005**, *76*, 126108.
(41) Kamphus, M.; Liu, N. N.; Atakan, B.; Qi, F.; McIlroy, A. *Proc. Combust. Inst.* **2003**, *29*, 2627.
(42) Li, Z.; Anderson, S. L. *J. Phys. Chem. A* **1998**, *102*, 9202.
(43) Geankoplis, C. J. *Transport Processes and Unit Operations*, 3rd ed.; PTR Prentice Hall: Englewood Cliffs, NJ, 1993.
(44) Linstrom, P. J.; Mallard, W. G. NIST Chemistry Webbook; National Institute of Standard and Technology: Gaithersburg, MD, 2005 (http://webbook.nist.gov/chemistry/).
(45) Cool, T. A.; Nakajima, K.; Taatjes, C. A.; McIlroy, A.; Westmoreland, P. R.; Law, M. E.; Morel, A. *Proc. Combust. Inst.* **2005**, *30*, 1681.
(46) Robinson, J. C.; Sveum, N. E.; Neumark, D. M. *Chem. Phys. Let.* **2004**, *350*, 601.
(47) Cool, T. A.; Wang, J.; Nakajima, K.; Taatjes, C. A.; McIlroy, A. *Int. J. Mass Spectrom.* **2005**, *247*, 18.
(48) Kanno, N.; Tonokura, K. *Appl. Spectrosc.* **2007**, *61*, 896.
(49) Wang, J.; Yang, B.; Cool, T. A.; Hansen, N.; Kasper, T. *Int. J. Mass Spectrom.* **2008**, *269*, 210.
(50) Xia, W. S.; Zhu, R. S.; Lin, M. C.; Mebel, A. M. *Faraday Discuss.* **2001**, *119*, 191.
(51) Zumdahl, S. S. *Chemistry*, 3rd ed.; D. C. Heath and Co.: Lexington, MA, 1993.
(52) Zhang, T. C.; Zhang, L. D.; Wang, J.; Yuan, T.; Hong, X.; Qi, F. *J. Phys. Chem. A* **2008**, *112*, 10495.

JP803622W